Published in final edited form as:
Biomaterials. 2010 September ; 31(25): 6502–6510. doi:10.1016/j.biomaterials.2010.05.017.

An injectable calcium phosphate-alginate hydrogel-umbilical cord mesenchymal stem cell paste for bone tissue engineering

Liang Zhao[1,#], **Michael D. Weir**[1,#], and **Hockin H. K. Xu**[1,2,3,4,*]

[1]Department of Endodontics, Prosthodontics and Operative Dentistry University of Maryland Dental School, Baltimore, MD 21201

[2]Center for Stem Cell Biology & Regenerative Medicine University of Maryland School of Medicine, Baltimore, MD 21201

[3]Member, University of Maryland Marlene and Stewart Greenebaum Cancer Center

[4]Department of Mechanical Engineering, University of Maryland, Baltimore County, MD 21250

Abstract

The need for bone repair has increased as the population ages. Stem cell-scaffold approaches hold immense promise for bone tissue engineering. However, currently, preformed scaffolds for cell delivery have drawbacks including the difficulty to seed cells deep into the scaffold, and inability for injection in minimally invasive surgeries. Current injectable polymeric carriers and hydrogels are too weak for load-bearing orthopedic application. The objective of this study was to develop an injectable and mechanically-strong stem cell construct for bone tissue engineering. Calcium phosphate cement (CPC) paste was combined with hydrogel microbeads encapsulating human umbilical cord mesenchymal stem cells (hUCMSCs). The hUCMSC-encapsulating composite paste was fully injectable under small injection forces. Cell viability after injection matched that in hydrogel without CPC and without injection. Mechanical properties of the construct matched the reported values of cancellous bone, and were much higher than previous injectable polymeric and hydrogel carriers. hUCMSCs in the injectable constructs osteodifferentiated, yielding high alkaline phosphatase, osteocalcin, collagen type I, and osterix gene expressions at 7 d, which were 50–70 fold higher than those at 1 d. Mineralization by the hUCMSCs at 14 d was 100-fold that at 1 d. In conclusion, a fully-injectable, mechanically-strong, stem cell-CPC scaffold construct was developed. The encapsulated hUCMSCs remained viable, osteodifferentiated, and synthesized bone minerals. The new injectable stem cell construct with load-bearing capability may enhance bone regeneration in minimally-invasive and other orthopedic surgeries.

Keywords

Injectable scaffold; umbilical cord stem cells; calcium phosphate cement; minimally invasive; osteogenic differentiation; load-bearing; bone tissue engineering

[*]Correspondence: Hockin Xu, Professor Department of Endodontics, Prosthodontics and Operative Dentistry, Dental School Center for Stem Cell Biology & Regenerative Medicine, School of Medicine University of Maryland Baltimore, MD 21201 hxu@umaryland.edu Phone: 410-706-7047 Fax: 410-706-3028.
[#]These two authors contributed equally to this work.

1. Introduction

Human bone marrow mesenchymal stem cells (hBMSCs) can differentiate into osteoblasts, adipocytes, chondrocytes, myoblasts, neurons and fibroblasts [1–4]. hBMSCs can be harvested from the patient, expanded in culture, induced to differentiate and combined with a scaffold to repair bone defects [5–8]. However, autogenous hBMSCs require an invasive procedure and have lower self-renewal potential with aging. Recently, human umbilical cord mesenchymal stem cells (hUCMSCs) were derived for tissue engineering [9–14]. Umbilical cords can provide an inexpensive and inexhaustible stem cell source, without the invasive procedure of hBMSCs, and without the controversies of embryonic stem cells (hESCs). hUCMSCs are primitive MSCs, exhibit a high plasticity and developmental flexibility, and appear to cause no immunorejection *in vivo* [10]. Recently, hUCMSCs were cultured with tissue culture plastic [11], polymer scaffolds [14], and calcium phosphate scaffolds for tissue engineering [15–17].

Calcium phosphate (CaP) scaffolds are important for bone repair because they are bioactive, mimic the bone minerals, and can bond to neighboring bone, in contrast to bioinert implants that can form undesirable fibrous capsules [18–20]. The CaP minerals provide a preferred substrate for cell attachment and expression of osteoblast phenotype [21,22]. However, for preformed bioceramic scaffolds to fit in a bone cavity, the surgeon needs to machine the graft or carve the surgical site, leading to increases in bone loss, trauma, and surgical time [1]. Preformed scaffolds have other drawbacks including the difficulty in seeding cells deep into the scaffold, and inability for injection in minimally-invasive surgeries [1,8]. Injectable scaffolds for cell delivery are advantageous because they can: (i) shorten the surgical operation time; (ii) minimize the damaging of large muscle retraction; (iii) reduce postoperative pain and scar size; (iv) achieve rapid recovery; and (v) reduce cost. Several injectable hydrogel and polymer carriers were meritorious for cell delivery [8,23]. However, current injectable carriers cannot be used in load-bearing repairs [8,23]. For example, it was concluded that “Hydrogel scaffolds … do not possess the mechanical strength to be used in load bearing applications” [23]. Mechanical properties are of crucial importance for the regeneration of load-bearing tissues such as bone, to withstand stresses to avoid scaffold fracture, and to maintain the structure to define the shape of the regenerated tissue. However, to date, an injectable, bioactive, and strong scaffold for stem cell encapsulation and bone engineering is yet to be developed.

Calcium phosphate cements (CPCs) can set *in situ* to form a bioactive scaffold that bonds to bone [24–27]. The first CPC was approved by the Food and Drug Administration (FDA) in 1996 for craniofacial repairs [24,28–30]. CPC has excellent osteoconductivity, is bioresorbable and can be replaced by new bone [28–30]. In previous studies, alginate hydrogel beads [17,31,32] and tubular hydrogels [33] were used to encapsulate cells in CPC. The hydrogel would protect the cells during the CPC mixing and setting reaction. Once the CPC has set, the hydrogel would dissolve and release the cells throughout the entire CPC scaffold, while concomitantly creating macroporosity. However, the hydrogel beads had diameters of 2–3 mm, hence the CPC-beads paste was not suitable for injection in minimally-invasive surgeries.

Therefore, the objective of this study was to develop a novel injectable and mechanically-strong stem cell construct, using CPC paste containing small microbeads of hydrogel for bone tissue engineering. It was hypothesized that: (1) CPC containing hUCMSC-encapsulating microbeads is fully injectable and mechanically strong, while that with large beads of previous studies is weak and not injectable; (2) Mechanical properties of the construct can be improved via chitosan and fibers, while maintaining the injectability for the paste; (3) The injection process does not harm the hUCMSCs in the paste; (4) hUCMSCs in

microbead-CPC constructs can remain viable, and be able to osteodifferentiate and synthesize bone minerals.

2. Materials and methods

2.1 Encapsulating hUCMSCs in alginate hydrogel beads

Alginate was used to encapsulate and protect the cells, selected because it is non-cytotoxic and can form a crosslinked gel under mild conditions [34]. Alginate is a natural polysaccharide extracted from seaweed. A 1.2% (mass fraction) sodium alginate solution was prepared by dissolving alginate (MW = 75,000 to 220,000 g/mol, ProNova, Norway) in saline (155 mmol/L NaCl) [31,32].

hUCMSCs were generously provided by Dr. M. S. Detamore (University of Kansas, Lawrence, KS). hUCMSCs were harvested from the Wharton's jelly of umbilical cords as described previously [9,14]. Briefly, umbilical cords were obtained from an obstetrician and incubated in a collagenase type I solution containing collagenase type I (300 U/mL), hyaluronidase (1 mg/mL) and calcium chloride (3 mM) for 30 min at 37 °C. The cords were minced and plated in a modified Dulbecco's modified Eagle's medium (DMEM) for 1 week [12]. The cord remnants were then removed and the attached cells were harvested.

The use of hUCMSCs was approved by the University of Maryland. Cells were cultured in a low-glucose DMEM with 10% fetal bovine serum (FBS) and 1% penicillin/streptomycin (PS) (Invitrogen, Carlsbad, CA) (control media) [15]. At 80–90% confluence, hUCMSCs were detached by trypsin and passaged. Passage 4 hUCMSCs were used for the experiments. The osteogenic media contained 100 nM dexamethasone, 10 mM β-glycerophosphate, 0.05 mM ascorbic acid, and 10 nM 1α,25-Dihydroxyvitamin (Sigma) [14,17].

hUCMSCs were encapsulated in alginate at a density of 1 million cells/mL of alginate solution [17]. Bead formation was accomplished by extruding alginate-cell droplets through a syringe into a well of 100 mmol/L calcium chloride solution. The alginate droplets crosslinked and formed beads. This resulted in beads of 2–3 mm in diameter, which were the same as those synthesized in previous studies [17,31,32]. These beads are referred to as “large beads”.

To improve the injectability, hUCMSC-encapsulating microbeads were developed in the present study. The alginate-cell solution was loaded into a syringe which was placed into a syringe pump and connected to a bead-generating device (Var J1, Nisco, Zurich, Switzerland), as shown schematically in Fig. 1A. Nitrogen gas was fed to the gas inlet and a pressure of 10 psi was established to form a coaxial air flow to break up the alginate droplets. This produced small alginate beads. A microscope (Eclipse TE-2000S, Nikon, Melville, NY) was used to measure the sizes of the beads. These beads are designated as “microbeads”.

2.2 CPC, chitosan, and degradable fibers

CPC consisted of tetracalcium phosphate [TTCP: $Ca_4(PO_4)_2O$] and dicalcium phosphate anhydrous (DCPA: $CaHPO_4$) [29,30]. TTCP was synthesized from a solid-state reaction between DCPA and $CaCO_3$, then ground in a blender to obtain particle sizes of 1–80 μm (median = 17 μm). DCPA was ground to obtain particle sizes of 0.4–3.0 μm (median = 1.0 μm). The TTCP and DCPA powders were mixed at a molar ratio of 1:1 to form the CPC powder.

Chitosan rendered CPC fast-setting and strong [35]. Chitosan and its derivatives are natural biopolymers that are biodegradable and osteoconductive [36]. Chitosan lactate (Vanson,

Redmond, WA) was mixed with water at a chitosan/(chitosan + water) mass fraction of 15%, which was termed “chitosan liquid” [37]. An absorbable suture fiber (Vicryl, polyglactin 910, Ethicon, Somerville, NJ) was used due to its relatively high strength [38]. The fiber was cut to a length of 3 mm so that the CPC-fiber paste was injectable, based on a pilot study.

2.3 Injectability

A 10 mL syringe (Free-Flo, Kerr, Romulus, MI) was used with a 10-gauge needle having an inner diameter of 2.7 mm [39,40]. The 10-gauge needle was similar to spinal needles used in the augmentation of osteoporotic vertebrae and the management of vertebral compression fractures [41]. The CPC paste was mixed and filled into the syringe which was pressed via a computer-controlled Universal Testing Machine (MTS, Eden Prairie, MN). The compression was started and the paste was extruded until either the paste was entirely extruded, or a maximum force of 100 N was reached [40]. The percentage of paste extruded was determined as the mass of the extruded paste divided by the original mass of the paste in the syringe [39]. The injection force was recorded and the maximum force was used as the injection force [39].

Four constructs were tested for injectability, all at a CPC powder to liquid ratio of 2/1: (1) CPC with water (control); (2) CPC with water + 50% volume fraction of hydrogel microbeads (CPC-microbeads); (3) CPC with chitosan + 50% microbeads (CPC-chitosan-microbeads); (4) CPC with chitosan + 50% microbeads + 20% fibers (CPC-chitosan-fiber-microbeads).

The microbead volume fraction of 50% was selected because this could encapsulate a relatively large amount of cells, and create 50% macroporosity in CPC after bead dissolution. The 20% fiber volume fraction in CPC was selected because a preliminary study showed that CPC with 10–20% of fibers were readily injectable, while CPC with 25% fibers was difficult to inject. CPC with large beads, the same as those in previous studies [17,31,32], was not included here because it was difficult to mix the large beads homogeneously with the paste, the paste was difficult to inject, and the large beads broke when forced through the 10-gauge needle.

2.4 Mechanical testing

CPC specimen of 3 × 4 × 25 mm was set in a humidor for 4 h at 37 °C. The hardened specimen was demolded and immersed in the culture media for 1 d. A three-point flexural test was used to fracture the specimens on the Universal Testing Machine [42]. Flexural strength $S = 3F_{max}L/(2bh^2)$, where F_{max} is the maximum load on the load-displacement (F-d) curve, L is span, b is specimen width, and h is thickness. Elastic modulus $E = (F/d)\ (L^3/[4bh^3])$, where load F divided by displacement d is the slope. Work-of-fracture (toughness), WOF, was calculated as the area under the F-d curve divided by the specimen's cross-sectional area [38].

2.5 Viability of encapsulated hUCMSCs

hUCMSC viability was compared between: (1) cells in microbeads without injection, and (2) cells in microbeads in CPC-chitosan-fiber paste after injection. The purpose was to investigate if the paste mixing and injection process would harm the cells. Each injected CPC construct was set in a well at 37 °C for 30 min. Then, 2 mL of the osteogenic media was added to each well. After 1 d, the constructs were carefully broken and the cell-encapsulating microbeads were collected. Cells were stained with a live/dead kit (Invitrogen, Carlsbad, CA). The percentage of live cells was: $P_{Live} = N_{Live}/(N_{Live} + N_{Dead})$, where N_{Live} = the number of live cells, and N_{Dead} = the number of dead cells [43]. The live cell density,

D_{Live}, was calculated: $D_{Live} = N_{Live}/A$, where A is the area of the view field for N_{Live} [15,17].

Next, the culture was prolonged to 7 d and 14 d, and the effects of different compositions of the injectable construct were compared: (1) hUCMSCs in hydrogel microbeads alone; (2) hUCMSCs in microbeads in CPC; (3) hUCMSCs in microbeads in CPC-chitosan; (4) hUCMSCs in microbeads in CPC-chitosan-fiber paste. P_{Live} and D_{Live} were measured as described above.

2.6 Osteogenic differentiation of encapsulated hUCMSCs

For osteodifferentiation, three experiments were performed. Experiment I used the quantitative real-time reverse transcription polymerase chain reaction (qRT-PCR, 7900HT, Applied Biosystems, Foster City, CA). The encapsulated hUCMSCs were cultured in the constructs for 1, 4, 7 and 14 d. The total cellular RNA of the cells were extracted with TRIzol reagent (Invitrogen) and reverse-transcribed into cDNA using a High-Capacity cDNA Archive kit. TaqMan gene expression assay kits, including two pre-designed specific primers and probes, were used to measure the transcript levels of the proposed genes on human alkaline phosphatase (ALP, Hs00758162_m1), osteocalcin (OC, Hs00609452_g1), collagen type I (Coll I, Hs00164004), osterix (Hs00541729), and glyceraldehyde 3-phosphate dehydrogenase (GAPDH, Hs99999905). Relative expression for each target gene was evaluated using the 2-ΔΔCt method [44]. Ct values of target genes were normalized by the Ct of the TaqMan human housekeeping gene GAPDH to obtain the ΔCt values. The Ct of hUCMSCs cultured on tissue culture polystyrene in the control media for 1 d served as the calibrator [17].

Experiment II measured the hUCMSCs' synthesis of the ALP protein. The cell-encapsulating microbeads harvested were dissolved by 55 mmol/L sodium citrate tribasic solution (Sigma). A colorimetric p-nitrophenyl phosphate (pNPP) assay (Stanbio, Boerne TX) was used to measure the ALP activity. Normal control serum with a known concentration of ALP served as standard. A microplate reader (M5 SpectraMax, Molecular Devices, Sunnyvale, CA) was used and the ALP was normalized by the DNA content [17,43]. DNA was quantified using the Quant-iT PicoGreen Kit (Invitrogen) following standard protocols [17,43].

Experiment III examined the mineral synthesis by the encapsulated hUCMSCs. Minerals emit red fluorescence when stained with xylenol orange (Sigma). The minerals synthesized by the cells in the hydrogel microbeads harvested from the constructs were stained and examined using both phase contrast and fluorescence images. Following a previous study [17], the mineral area percentage was calculated as $A_{Mineral}/A_{Total}$, where $A_{Mineral}$ is the area of mineralization (red fluorescence), and A_{Total} is the total area of the field of view of the image.

The cells were typically cultured for 1, 7, and 14 d following previous studies [32,37,43]. An exception was made for the RT-PCR experiment, where day-4 was also studied. This is because genetic expression occurs in the early stage of osteodifferentiation. A previous study observed a high ALP expression at 4 d [44]. Another exception was made for the ALP protein synthesis by the cells, where day-1 was not done but day-21 was added. This is because the ALP protein synthesis by the cells occurs at a later time; it peaked at 14-d in previous studies [17,43]. Doing 7, 14 and 21 d would help determine if the ALP protein synthesis indeed peaks at 14 d.

One-way and two-way ANOVA were performed to detect significant effects of the variables. Tukey's multiple comparison tests were used at a p value of 0.05.

3. Results

Fig. 1B shows the diameter histogram of the hUCMSC-encapsulating hydrogel microbeads, based on the measurement of 211 randomly-selected microbeads. The diameter ranged from 73 to 465 μm, and the mean diameter was 207 μm.

The mechanical properties of CPC constructs containing 50% of hUCMSC-encapsulating hydrogel beads are plotted in Fig. 1C–E. Compared to the large beads similar to those in previous studies, the use of the new microbeads increased the flexural strength of the stem cell-CPC construct by 4-fold, elastic modulus by 5-fold, and work-of-fracture by 7-fold.

The injectability results are shown in Fig. 2. All the pastes were readily extruded at relatively small injection forces. Compared to CPC control (no chitosan, no beads, no fibers), CPC + 50% microbeads was extruded under a higher force ($p < 0.05$). Adding chitosan rendered the paste more cohesive, which was fully extruded at a much lower force ($p < 0.05$). Compared to CPC-microbeads, the injection force for CPC-chitosan-fiber-microbeads was similar ($p > 0.1$); therefore, adding chitosan and fibers for reinforcement did not compromise the injectability.

Mechanical properties of CPC containing 50% of hUCMSC-encapsulating microbeads are plotted in Fig. 3. Adding chitosan and fibers increased the load-bearing properties ($p < 0.05$). The CPC-chitosan-fiber-microbead construct reached a flexural strength of 4 MPa. Compared to CPC-microbeads, the strength of CPC-chitosan-fiber-microbeads was 3-fold higher, and WOF was 100-fold higher. Elastic modulus decreased because the polyglactin fibers were flexible and not stiff. The previously-reported strength and modulus for cancellous bone, injectable polymer and hydrogels for cell delivery are included in Fig. 3, as described in Discussion.

Fig. 4 compares the hUCMSCs in microbeads alone (without CPC and without injection), with those mixed in the CPC-chitosan-fiber paste and then injected. Both were cultured for 1 d and then stained. In (D) and (E), the percentage of live cells and cell density indicate that the paste mixing and injection process did not harm the encapsulated hUCMSCs.

When prolonged to 7 d and 14 d, the cells remained viable and the percentage of live cells was similar to those at 1 d ($p > 0.1$). For example, the percentage of live cells at 14 d was $(68 \pm 5)\%$ in microbeads alone, $(73 \pm 6)\%$ in microbeads in CPC, $(71 \pm 4)\%$ in CPC-chitosan, and $(71 \pm 6)\%$ in CPC-chitosan-fiber paste ($p > 0.1$). Therefore, compared to hUCMSCs in hydrogel microbeads without CPC, encapsulation in CPC did not compromise the cell viability.

In Fig. 5, the ALP gene expression was greatly increased at 7 d, and then slightly decreased at 14 d. The OC, collagen type I, and osterix expressions showed similar trends. Compared to hUCMSCs in microbeads without CPC, encapsulation in CPC did not adversely affect the ALP, OC, collagen I, and osterix ($p > 0.1$).

The ALP protein synthesis (Fig. 6) by the hUCMSCs peaked at 14 d ($p < 0.01$). The ALP activity at 14 d was about 6-fold higher than that at 7 d for all the constructs.

The mineral synthesis by hUCMSCs increased from 1 d, to 7 d, and 14 d (Fig. 7). This trend was the same in all four constructs. The stained mineral area percentage is plotted in (E). The staining areas at 14 d were nearly 100-fold those at 1 d. The incorporation of chitosan and fibers, which greatly increased the load-bearing capability of CPC, did not compromise the mineral synthesis of the hUCMSCs ($p > 0.1$).

4. Discussion

Hydroxyapatite and other CaP bioceramics are important for hard tissue repair because of their excellent biocompatibility [3,6,8,18–22]. When implanted in an osseous site, bone bioactive materials such as HA and other CaP implants and coatings provide an ideal environment for cellular reaction and colonization by osteoblasts. This leads to a tissue response termed osteoconduction in which bone grows on and bonds to the implant, promoting a functional interface. Many studies have improved HA and other CaP implants [3,6,8,18–22]. MSCs showed elevated levels of ALP when grown on 45S5 bioactive glass, as compared to tissue culture plastic [21]. An *in vivo* study showed that β-tricalcium phosphate mixed with hMSCs formed new bone in posterolateral spine fusion [45]. Calcium magnesium silicate induced proliferation and expression of ALP and OC *in vitro* [46]. hMSCs on HA had excellent osteoinduction [47], and porous HA scaffolds showed an enhancement of BMSC differentiation [48]. However, sintered HA implants are generally not resorbable. Another major disadvantage of current orthopaedic implants including sintered bioceramics is that they exist in hardened forms, require machining, and may leave gaps when fitted into a bone cavity [1].

CPC can self-set with intimate adaptation to complex-shaped cavities, can be easily shaped for esthetics in craniofacial repairs, and is osteoconductive and bioresorbable [24-30]. In previous studies, macroporous CPC was developed [30], fast-setting and washout-resistant CPC was formulated [35], and the load-bearing properties were improved [38]. Other studies focused on the injectability of CPCs, the incorporation of a polymeric drug and citric acid [8,26,49–52], and the use of TGF-β1 loaded gelatin microspheres [27]. Osteoblasts and BMSCs were cultured on CPC [15,37,43]. In recent studies, cells were encapsulated in alginate beads which were then mixed with CPC [17,31,32]. The cells were viable and able to osteodifferentiate [17]. However, the beads had diameters of 2–3 mm, the CPC-bead paste was difficult to be injected, and the CPC construct containing the large beads was mechanically weak.

The present study reports an injectable stem cell-CPC construct, via microbeads for hUCMSC encapsulation and absorbable fibers for reinforcement. Compared to previous CPC containing large beads [17,31,32], the CPC-microbead-stem cell construct had higher mechanical properties (Fig. 1C–E), and was readily injectable (Fig. 2). When a powder and a liquid were mixed into a paste and injected through a cannula, a filter-pressing phenomenon often occurred in which the liquid was pushed out but a major portion of the powder remained inside the syringe, leading to a phase separation of the liquid and the solid [26,49,52]. The addition of chitosan formed a viscous and cohesive paste, and made it more difficult for the solid and liquid phases to separate, thereby improving the injectability of the paste. This resulted in the injection force of CPC-chitosan-fiber-microbeads to be statistically similar to that of CPC-microbeads without fibers (Fig. 2B), while the former was much stronger (Fig. 3). Therefore, the incorporation of chitosan and fibers greatly increased the strength and toughness for the stem cell construct, without compromising the injectability, compared to CPC-microbeads without fibers.

A previous study reported a tensile strength of 3.5 MPa for cancellous bone [53]. Other studies reported that the strength was 0.7 MPa for injectable polymeric carriers for cell delivery [54], and 0.1 MPa for hydrogels [55,56]. The elastic modulus was 0.30 GPa for cancellous bone [57], 0.008 GPa for an injectable polymeric carrier [54], and 0.0001 GPa for hydrogels [55,56]. These previous injectable carriers are meritorious for tissue engineering in non-load-bearing locations. In comparison, the new injectable stem cell-CPC-fiber construct are much stronger (Fig. 3), and may be useful for a wide range of craniofacial and orthopedic applications.

hUCMSCs are promising to be an inexhaustible and low-cost alternative to the gold-standard hBMSCs, which require an invasive procedure to harvest. ALP, osteocalcin, collagen I, and osterix gene expressions play important roles in the osteogenic differentiation of MSCs [58–61]. In the present study on injectable hUCMSC-CPC constructs, the ALP, OC, collagen I, and osterix gene expressions all peaked at 7 d. The ALP activity via the pNPP assay peaked at 14 d. This is because at the early stage of differentiation, the genetic expression of ALP is upregulated. This sets off a cascade of events which lead to the production of the ALP protein. The RT-PCR method measures the gene expression of ALP which occurs at an earlier time, while the pNPP assay measures the activity of the ALP protein which occurs at a later time. ALP is an enzyme expressed by MSCs during osteogenesis and is a well-defined marker for their differentiation [21,60,61]. Previous studies showed that the ALP activity peaked at 14 d [60,61], consistent with the present study. Regarding the OC expression, a previous study showed that it peaked at 8 d [44], which is consistent with the OC peak at 7 d of the present study. Furthermore, the hUCMSCs in all constructs synthesized bone minerals as shown by the xylenol orange staining. In a previous study, the cell-synthesized minerals were shown to be a poorly-crystalline apatite similar to those in bone [17]. These results demonstrate that the hUCMSCs encapsulated in the microbrads in the injectable CPC, in CPC-chitosan, and in CPC-chitosan-fiber constructs have all differentiated into the osteogenic lineage and synthesized bone minerals.

5. Conclusions

A fully-injectable, stem cell-encapsulating scaffold was developed with mechanical strength matching that of cancellous bone. The hUCMSC-microbead-CPC construct was much stronger than previous CPC containing large alginate beads which was not injectable. The new hUCMSC-microbead-CPC construct was fully injectable under a small injection force. The strength and modulus of the new stem cell-CPC construct were much higher than previous injectable polymers and hydrogels for cell delivery. The injection in this study did not harm the hUCMSC viability. The encapsulated hUCMSCs differentiated into the osteogenic lineage, with highly elevated ALP, OC, collagen I and osterix expressions, ALP protein synthesis, and mineralization. The osteogenic markers and mineralization of hUCMSCs in the injectable constructs matched those in hydrogel without CPC. These results support the use of hUCMSCs as an inexhaustible and low-cost alternative to the gold-standard hBMSCs, which require an invasive procedure to harvest. Furthermore, these results show that the injectable, strong, stem cell-CPC scaffold is promising for minimally-invasive and other orthopedic surgeries.

Acknowledgments

We are indebted to Prof. M. S. Detamore at the University of Kansas, Lawrence, KS for kindly providing the hUCMSCs. We thank Drs. L. C. Chow, S. Takagi and A. A. Giusseppetti at the Paffenbarger Research Center, Dr. Carl G. Simon at the National Institute of Standards and Technology, and Dr. John Fisher at the University of Maryland for discussions and help. This study was supported by NIH R01 grants DE14190 and DE17974 (HX), Maryland Stem Cell Research Fund (HX), and the University of Maryland Dental School.

References

[1]. Laurencin CT, Ambrosio AMA, Borden MD, Cooper JA. Tissue engineering: Orthopedic applications. Annual Rev Biomed Eng 1999;1:19–46. [PubMed: 11701481]

[2]. Sikavitsas VI, Bancroft GN, Holtorf HL, Jansen JA, Mikos AG. Mineralized matrix deposition by marrow stromal osteoblasts in 3D perfusion culture increases with increasing fluid shear forces. Proc Natl Acad Sci USA 2003;100:14683–14688. [PubMed: 14657343]

[3]. Yao J, Radin S, Reilly G, Leboy PS, Ducheyne P. Solution-mediated effect of bioactive glass in poly (lactic-co-glycolic acid)-bioactive glass composites on osteogenesis of marrow stromal cells. J Biomed Mater Res 2005;75A:794–801.

[4]. Mao JJ, Giannobile WV, Helms JA, Hollister SJ, Krebsbach PH, Longaker MT, et al. Craniofacial tissue engineering by stem cells. J Dent Res 2006;85:966–979. [PubMed: 17062735]

[5]. Datta N, Pham QP, Sharma U, Sikavitsas VI, Jansen JA, Mikos AG. *In vitro* generated extracellular matrix and fluid shear stress synergistically enhance 3D osteoblastic differentiation. Proc Natl Acad Sci USA 2006;103:2488–2493. [PubMed: 16477044]

[6]. Silva GA, Coutinho OP, Ducheyne P, Reis RL. Materials in particulate form for tissue engineering, Part 2: Applications in bone (review). J Tissue Eng Regen Med 2007;1:97–109. [PubMed: 18038398]

[7]. Mao, JJ.; Vunjak-Novakovic, G.; Mikos, AG.; Atala, A. Regenerative medicine: Translational approaches and tissue engineering. Artech House; Boston and London: 2007.

[8]. Kretlow JD, Young S, Klouda L, Wong M, Mikos AG. Injectable biomaterials for regenerating complex craniofacial tissues. Adv Mater 2009;21:3368–3393. [PubMed: 19750143]

[9]. Wang HS, Hung SC, Peng ST. Mesenchymal stem cells in the Wharton's jelly of the human umbilical cord. Stem Cells 2004;22:1330–1337. [PubMed: 15579650]

[10]. Can A, Karahuseyinoglu S. Concise review: Human umbilical cord stroma with regard to the source of fetus-derived stem cells. Stem Cells 2007;25:2886–2895. [PubMed: 17690177]

[11]. Baksh D, Yao R, Tuan RS. Comparison of proliferative and multilineage differentiation potential of human mesenchymal stem cells derived from umbilical cord and bone marrow. Stem Cells 2007;25:1384–1392. [PubMed: 17332507]

[12]. Bailey MM, Wang L, Bode CJ, Mitchell KE, Detamore MS. A comparison of human umbilical cord matrix stem cells and temporomandibular joint condylar chondrocytes for tissue engineering temporomandibular joint condylar cartilage. Tissue Eng 2007;13:2003–2010. [PubMed: 17518722]

[13]. Karahuseyinoglu S, Kocaefe C, Balci D, Erdemli E, Can A. Functional structure of adipocytes differentiated from human umbilical cord stroma-derived stem cells. Stem Cells 2008;26:682–691. [PubMed: 18192234]

[14]. Wang L, Singh M, Bonewald LF, Detamore MS. Signaling strategies for osteogenic differentiation of human umbilical cord mesenchymal stromal cells for 3D bone tissue engineering. J Tissue Eng Regen Med 2009;3:398–404. [PubMed: 19434662]

[15]. Zhao L, Burguera EF, Xu HHK, Amin N, Ryou H, Arola DD. Fatigue and human umbilical cord stem cell seeding characteristics of calcium phosphate-chitosan-biodegradable fiber scaffolds. Biomaterials 2010;31:840–847. [PubMed: 19850337]

[16]. Jäger M, Degistirici O, Knipper A, Fischer J, Sager M, Krauspe R. Bone healing and migration of cord blood-derived stem cells into a critical size femoral defect after xenotransplantation. J Bone Miner Res 2007;22:1224–1233. [PubMed: 17451370]

[17]. Zhao L, Weir MD, Xu HHK. Human umbilical cord stem cell encapsulation in calcium phosphate scaffolds for bone engineering. Biomaterials 2010;31:3848–3857. [PubMed: 20149437]

[18]. Ducheyne P, Qiu Q. Bioactive ceramics: the effect of surface reactivity on bone formation and bone cell function. Biomaterials 1999;20:2287–2303. [PubMed: 10614935]

[19]. Pilliar RM, Filiaggi MJ, Wells JD, Grynpas MD, Kandel RA. Porous calcium polyphosphate scaffolds for bone substitute applications – in vitro characterization. Biomaterials 2001;22:963–972. [PubMed: 11311015]

[20]. Foppiano S, Marshall SJ, Marshall GW, Saiz E, Tomsia AP. The influence of novel bioactive glasses on in vitro osteoblast behavior. J Biomed Mater Res 2004;71A:242–249.

[21]. Reilly GC, Radin S, Chen AT, Ducheyne P. Differential alkaline phosphatase responses of rat and human bone marrow derived mesenchymal stem cells to 45S5 bioactive glass. Biomaterials 2007;28:4091–4097. [PubMed: 17586040]

[22]. Deville S, Saiz E, Nalla RK, Tomsia AP. Freezing as a path to build complex composites. Science 2006;311:515–518. [PubMed: 16439659]

[23]. Drury JL, Mooney DJ. Review. Hydrogels for tissue engineering: scaffold design variables and applications. Biomaterials 2003;24:4337–4351. [PubMed: 12922147]

[24]. Brown, WE.; Chow, LC. A new calcium phosphate water setting cement. In: Brown, PW., editor. Cements research progress. Am Ceram Soc.; Westerville, OH: 1986. p. 352-379.

[25]. Barralet JE, Gaunt T, Wright AJ, Gibson IR, Knowles JC. Effect of porosity reduction by compaction on compressive strength and microstructure of calcium phosphate cement. J Biomed Mater Res 2002;63B:1–9. [PubMed: 11787022]

[26]. Bohner M, Baroud G. Injectability of calcium phosphate pastes. Biomaterials 2005;26:1553–1563. [PubMed: 15522757]

[27]. Link DP, van den Dolder J, van den Beucken JJ, Wolke JG, Mikos AG, Jansen JA. Bone response and mechanical strength of rabbit femoral defects filled with injectable CaP cements containing TGF-β1 loaded gelatin microspheres. Biomaterials 2008;29:675–682. [PubMed: 17996293]

[28]. Shindo ML, Costantino PD, Friedman CD, Chow LC. Facial skeletal augmentation using hydroxyapatite cement. Arch Otolaryngol Head Neck Surg 1993;119:185–190. [PubMed: 8427682]

[29]. Friedman CD, Costantino PD, Takagi S, Chow LC. BoneSource hydroxyapatite cement: a novel biomaterial for craniofacial skeletal tissue engineering and reconstruction. J Biomed Mater Res 1998;43B:428–432. [PubMed: 9855201]

[30]. Xu, HHK.; Chow, LC.; Takagi, S.; Eichmiller, FC. Self-hardening calcium phosphate materials with high resistance to fracture, controlled strength histories and tailored macropore formation rates. U.S. Patent. No. 6,955,716. 2005.

[31]. Simon CG Jr. Guthrie WF, Wang FW. Cell seeding into calcium phosphate cement. J Biomed Mater Res 2004;68A:628–639.

[32]. Weir MD, Xu HHK, Simon CG Jr. Strong calcium phosphate cement-chitosan-mesh construct containing cell-encapsulating hydrogel beads for bone tissue engineering. J Biomed Mater Res 2006;77A:487–496.

[33]. Xu, HHK.; Weir, MD. Three-dimensional cell protector/pore architecture formation for bone and tissue constructs. U.S. Patent. No. 11/132,028. 2009. allowed Nov. 25

[34]. Koch S, Schwinger C, Kressler J, Heinzen C, Rainov NG. Alginate encapsulation of genetically engineered mammalian cells: comparison of production devices, methods and microcapsule characteristics. J Microencapsul 2003;20:303–316. [PubMed: 12881112]

[35]. Xu HHK, Takagi S, Quinn JB, Chow LC. Fast-setting and anti-washout calcium phosphate scaffolds with high strength and controlled macropore formation rates. J Biomed Mater Res 2004;68A:725–734.

[36]. Muzzarelli RAA, Biagini G, Bellardini M, Simonelli L, Castaldini C, Fraatto G. Osteoconduction exerted by methylpyrolidinone chitosan in dental surgery. Biomaterials 1993;14:39–43. [PubMed: 8425023]

[37]. Xu HHK, Simon CG Jr. Fast setting calcium phosphate-chitosan scaffold: mechanical properties and biocompatibility. Biomaterials 2005;26:1337–1348. [PubMed: 15482821]

[38]. Xu HHK, Simon CG Jr. Self-hardening calcium phosphate composite scaffold for bone tissue engineering. J Orthopaedic Res 2004;22:535–543.

[39]. Burguera EF, Xu HHK, Weir MD. Injectable and rapid-setting calcium phosphate bone cement with dicalcium phosphate dihydrate. J Biomed Mater Res 2006;77B:126–134.

[40]. Xu HHK, Weir MD, Burguera EF, Fraser AM. Injectable and macroporous calcium phosphate cement scaffold. Biomaterials 2006;27:4279–4287. [PubMed: 16650891]

[41]. Bai B, Jazrawi LM, Kummer FJ, Spivak JM. The use of an injectable, biodegradable calcium phosphate bone substitute for the prophylactic augmentation of osteoporotic vertebrae and the management of vertebral compression fractures. Spine 1999;24:1521–1526. [PubMed: 10457570]

[42]. American Society for Testing and Materials. ASTM D 790-03: Standard test methods for flexural properties of unreinforced and reinforced plastic and electrical insulating materials. ASTM International; West Conshohocken, PA: 2004.

[43]. Moreau JL, Xu HHK. Mesenchymal stem cell proliferation and differentiation on an injectable calcium phosphate-chitosan composite scaffold. Biomaterials 2009;30:2675–2682. [PubMed: 19187958]

[44]. Kim K, Dean D, Mikos AG, Fisher JP. Effect of initial cell seeding density on early osteogenic signal expression of rat bone marrow stromal cells cultured on cross-linked poly(propylene fumarate) disks. Biomacromolecules 2009;10:1810–1817.

[45]. Orii H, Sotome S, Chen J, Wang J, Shinomiya K. Beta-tricalcium phosphate (beta-TCP) graft combined with bone marrow stromal cells (MSCs) for posterolateral spine fusion. J Med Dent Sci 2005;52:51–57. [PubMed: 15868741]

[46]. Sun H, Wu C, Dai K, Chang J, Tang T. Proliferation and osteoblastic differentiation of human bone marrow-derived stromal cells on akermanite-bioactive ceramics. Biomaterials 2006;27:5651–5657. [PubMed: 16904740]

[47]. Nair MB, Bernhardt A, Lode A, Heinemann C, Thieme S, Hanke T, et al. A bioactive triphasic ceramic-coated hydroxyapatite promotes proliferation and osteogenic differentiation of human bone marrow stromal cells. J Biomed Mater Res 2009;90A:533–542.

[48]. Detsch R, Uhl F, Deisinger U, Ziegler G. 3D-Cultivation of bone marrow stromal cells on hydroxyapatite scaffolds fabricated by dispense-plotting and negative mould technique. J Mater Sci: Mater Med 2008;19:1491–1496. [PubMed: 17990079]

[49]. Ginebra MP, Rilliard A, Fernández E, Elvira C, Román JS, Planell JA. Mechanical and rheological improvement of a calcium phosphate cement by the addition of a polymeric drug. J Biomed Mater Res 2001;57:113–118. [PubMed: 11416857]

[50]. Sarda S, Fernández E, Nilsson M, Balcells M, Planell JA. Kinetic study of citric acid influence on calcium phosphate bone cement as water-reducing agent. J Biomed Mater Res 2002;61:653–659. [PubMed: 12115456]

[51]. Baroud G, Wu JZ, Bohner M, Sponagel S, Steffen T. How to determine the permeability for cement infiltration of osteoporotic cancellous bone. Med Eng Phys 2003;25:283–288. [PubMed: 12649012]

[52]. Gbureck U, Barralet JE, Spatz K, Grover LM, Thull R. Ionic modification of calcium phosphate cement viscosity: Part I: hypodermic injection and strength improvement of apatite cement. Biomaterials 2004;25:2187–2195. [PubMed: 14741634]

[53]. Damien CJ, Parsons JR. Bone graft and bone graft substitutes: A review of current technology and applications. J Appl Biomater 1991;2:187–208. [PubMed: 10149083]

[54]. Shi X, Sitharaman B, Pham QP, Liang F, Wu K, Billups WE, et al. Fabrication of porous ultra-short single-walled carbon nanotube nanocomposite scaffolds for bone tissue engineering. Biomaterials 2007;28:4078–4090. [PubMed: 17576009]

[55]. Drury JL, Dennis RG, Mooney DJ. The tensile properties of alginate hydrogels. Biomaterials 2004;25:3187–3199. [PubMed: 14980414]

[56]. Kuo CK, Ma PX. Ionically crosslinked alginate hydrogels as scaffolds for tissue engineering: Part I. Structure, gelation rate and mechanical properties. Biomaterials 2001;22:511–521. [PubMed: 11219714]

[57]. O'Kelly K, Tancred D, McCormack B, Carr A. A quantitative technique for comparing synthetic porous hydroxyapatite structure and cancellous bone. J Mater Sci: Mater in Med 1996;7:207–213.

[58]. Lavery K, Hawley S, Swain P, Rooney R, Falb D, Alaoui-Ismaili MH. New insights into BMP-7 mediated osteoblastic differentiation of primary human mesenchymal stem cells. Bone 2009;45:27–41. [PubMed: 19306956]

[59]. Zhang ZY, Teoh SH, Chong MS, Schantz JT, Fisk NM, Choolani MA, et al. Superior osteogenic capacity for bone tissue engineering of fetal compared with perinatal and adult mesenchymal stem cells. Stem cells 2009;27:126–137. [PubMed: 18832592]

[60]. Benoit DSW, Nuttelman CR, Collins SD, Anseth KS. Synthesis and characterization of a fluvastatin-releasing hydrogel delivery system to modulate hMSC differentiation and function for bone regeneration. Biomaterials 2006;27:6102–6110. [PubMed: 16860387]

[61]. Leach JK, Kaigler D, Wang Z, Krebsbach PH, Mooney DJ. Coating of VEGF-releasing scaffolds with bioactive glass for angiogenesis and bone regeneration. Biomaterials 2006;27:3249–3255. [PubMed: 16490250]

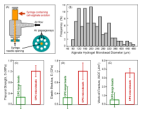

Figure [1].
Alginate microbead synthesis and mechanical properties of the constructs. (A) Schematic of the hUCMSC-encapsulating microbead synthesizer. (B) Microbead size. (C) Flexural strength, (D) elastic modulus, and (E) work-of-fracture (toughness) of CPC containing 50% of hUCMSC-encapsulating beads (mean ± sd; n = 5). The large beads were the same as those in previous studies [17,31,32]. The microbeads were made in this study.

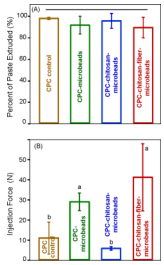

Figure [2].

Injectability of the hUCMSC-CPC constructs (mean ± sd; n = 3). (A) Percent of paste extruded. (B) Maximum injection force. The injection force for CPC-chitosan-fiber-microbeads was statistically similar ($p > 0.1$) to that for CPC-microbeads without fibers.

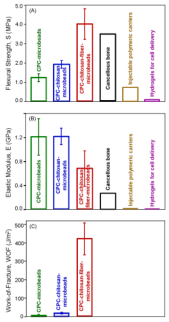

Figure [3].

Mechanical properties of the injectable stem cell constructs. Each specimen contained 50% by volume of microbeads that encapsulated 150,000 hUCMSCs. The strength and work-of-fracture (mean ± sd; n = 5) of the constructs were greatly increased via the incorporation of chitosan and fibers. Values for cancellous bone, injectable polymer, and hydrogels are obtained from the literature, as described in the Discussion section.

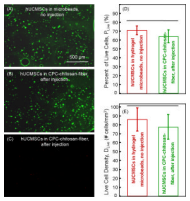

Figure [4].
hUCMSC viability without injection or after injection. (A) hUCMSCs in microbeads (without CPC, without injection). (B) hUCMSCs in microbeads after mixing with CPC-chitosan-fiber paste and after injection. Live cells (green) were numerous. Dead cells (red) were very few (C). (D) Percent of live cells (mean ± sd; n = 5). (E) Live cell density. The CPC mixing and injection process did not significantly harm the encapsulated hUCMSCs.

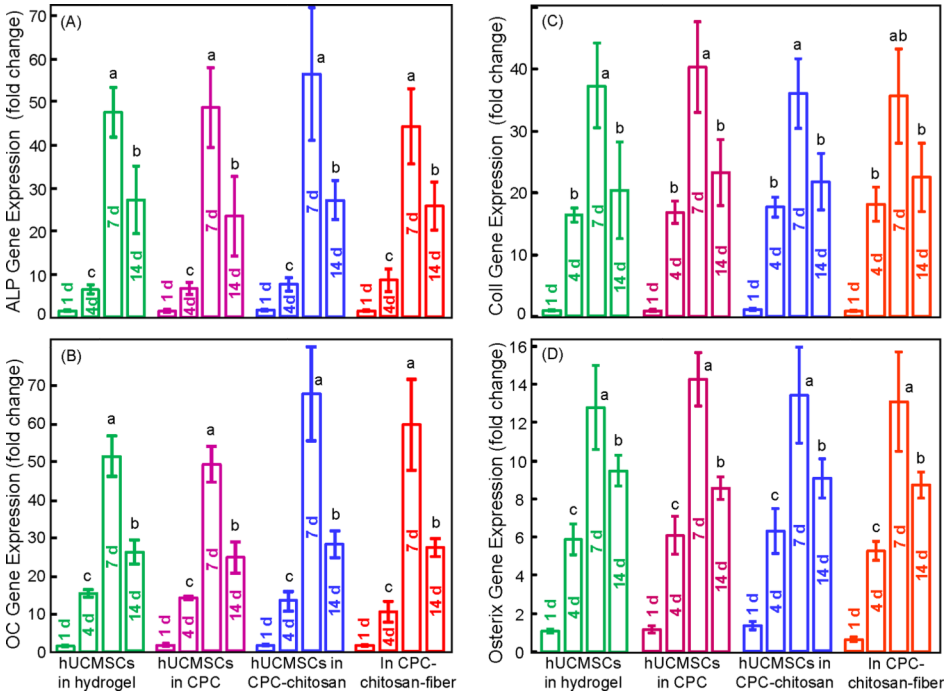

Figure [5].

Osteogenic differentiation of the encapsulated hUCMSCs. The RT-PCR results of (A) ALP, (B) OC, (C) collagen type I, and (D) osterix gene expressions (mean ± sd; n = 5). ALP, OC, collagen I and osterix were all greatly increased at 7 d, compared to those at 1 d. Encapsulation in CPC pastes did not adversely affect the bone marker expressions, compared to hUCMSCs in hydrogel without CPC.

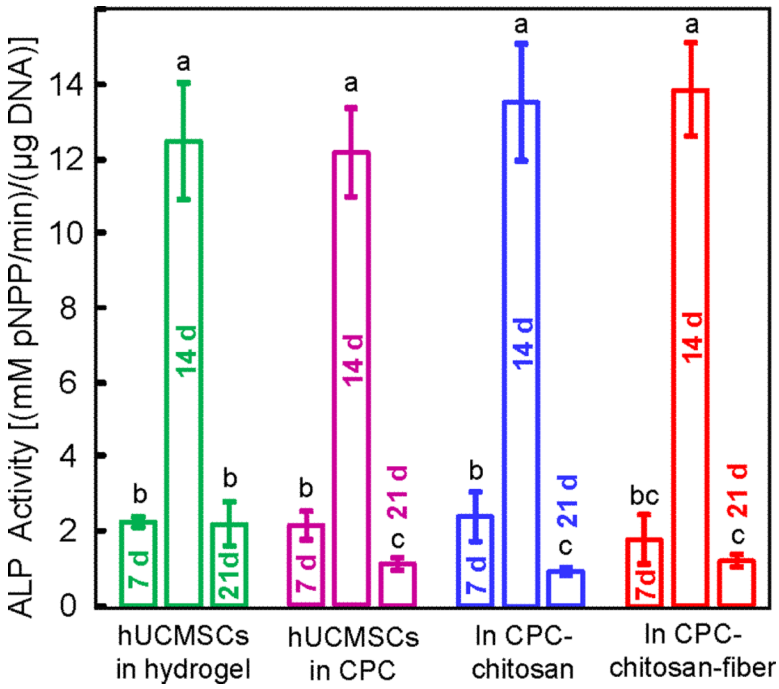

Figure [6].

Colorimetric pNPP assay of ALP protein synthesis by the encapsulated hUCMSCs. The ALP enzyme production greatly increased at 14 d over that at 7 d, and then decreased at 21 d (mean ± sd; n = 5). The ALP activity of hUCMSCs in all the injectable CPC-based constructs matched that in hydrogel microbeads without CPC.

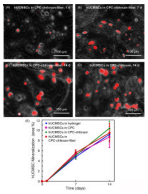

Figure [7].
Synthesis of bone minerals by the encapsulated hUCMSCs. (A–D) Mineral staining photos. Minerals emitted red fluorescence when stained with xylenol orange. The mineralization by hUCMSCs increased rapidly with time in all four constructs. (E) Mineral area fraction (mean ± sd; n = 5). hUCMSCs encapsulated in the injectable and mechanically-strong CPC-based constructs matched the mineralization in hydrogel without CPC.